

Electronic Supplementary Information

Enhanced Electrocatalytic Oxygen Evolution Reaction by Photothermal Effect and Its Induced Micro-electric Field

Feng Duan,^a Qian Zou,^a Junzhe Li,^a Xiaozhi Yuan,^a Xun Cui,^c Chuan Jing,^d Shengrong

Tao,^d Xijun Wei,^{*a} Huichao He^{*b} and Yingze Song^{*a}

^a*State Key Laboratory of Environment-Friendly Energy Materials, School of Materials and Chemistry, Engineering Research Center of Biomass Materials, Ministry of Education, Southwest University of Science and Technology, Mianyang 621010, P. R. China.*

^b*Institute of Environmental Energy Materials and Intelligent Devices, School of Metallurgy and Materials Engineering, Chongqing University of Science and Technology, Chongqing 401331, P. R. China.*

^c*State Key Laboratory of New Textile Materials and Advanced Processing Technologies, Wuhan Textile University, Wuhan 430200, P. R. China.*

^d*College of Science, Chongqing University of Posts and Telecommunications, Chongqing 400065, P. R. China*

*Email: xijunwei1992@swust.edu.cn (Xijun Wei)

*Email: hehuichao@cqust.edu.cn (Huichao He)

*Email: yzsng@swust.edu.cn (Yingze Song)

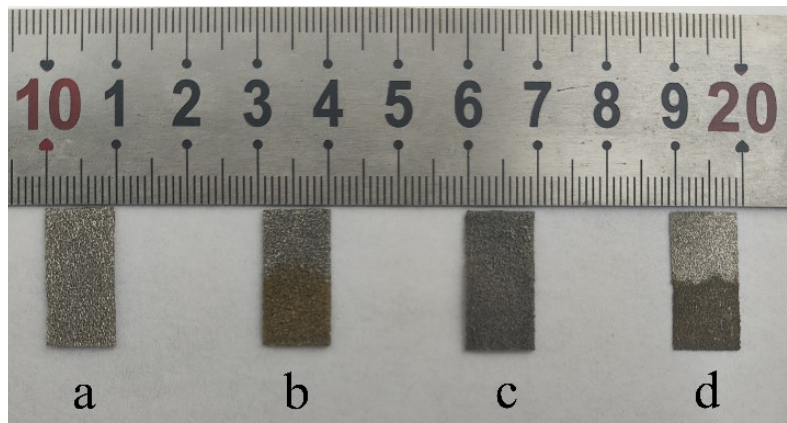


Fig. S1 The electrode pictures of (a) nickle foam (NF), (b) NiFe(OH)_y/NF, (c) NiS_x/NF and (d) NiS_x@NiFe(OH)_y/NF.

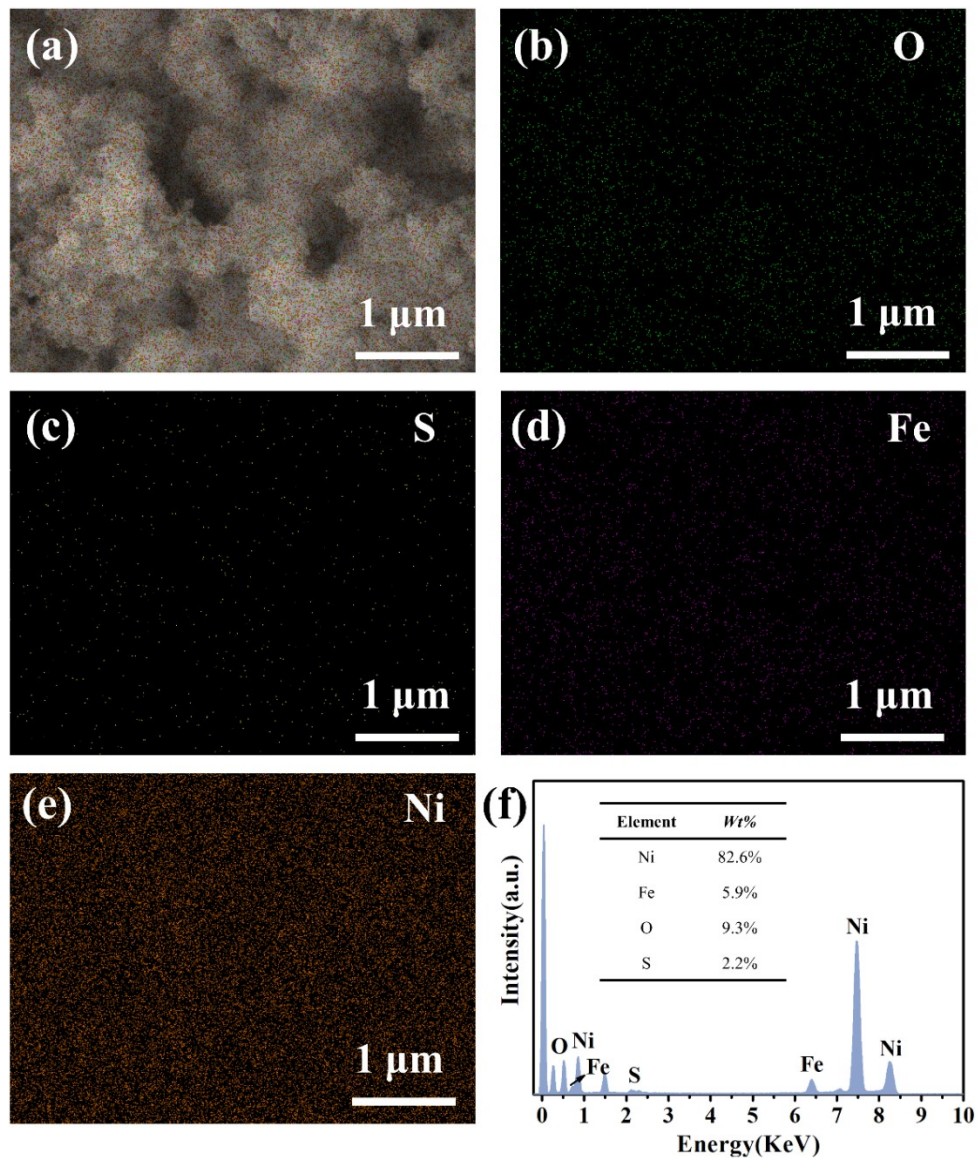


Fig. S2 (a)-(e) EDS mapping for $\text{NiS}_x@\text{NiFe}(\text{OH})_y/\text{NF}$, (f) EDS analysis result of $\text{NiS}_x@\text{NiFe}(\text{OH})_y/\text{NF}$.

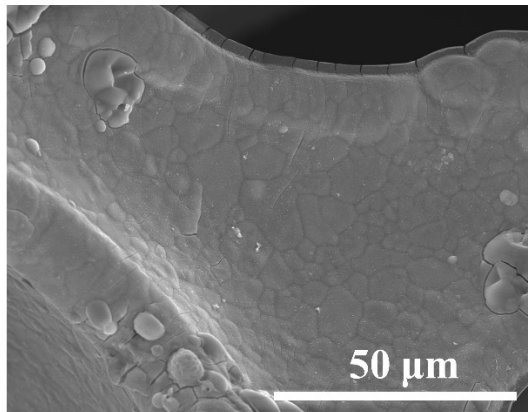


Fig. S3 SEM image of NiS_x/NF .

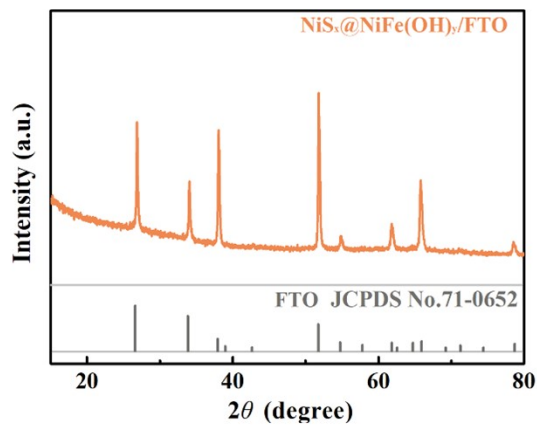


Fig. S4 XRD pattern of electrodeposited $\text{NiS}_x@\text{NiFe(OH)}_y$ on the fluorine-doped tin oxide ($\text{NiS}_x@\text{NiFe(OH)}_y/\text{FTO}$).

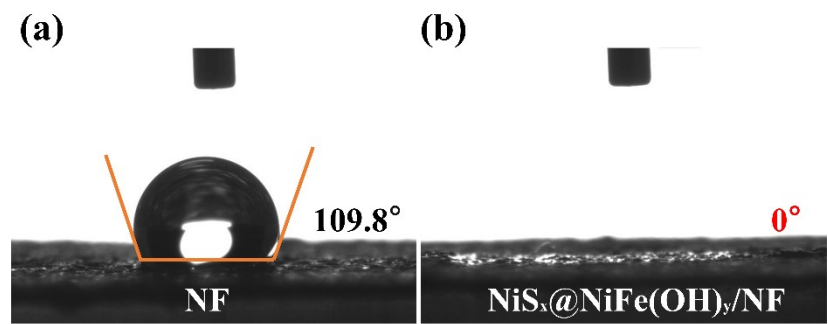


Fig. S5 The static droplet contact angles for (a) NF and (b) NiS_x@NiFe(OH)_y/NF.

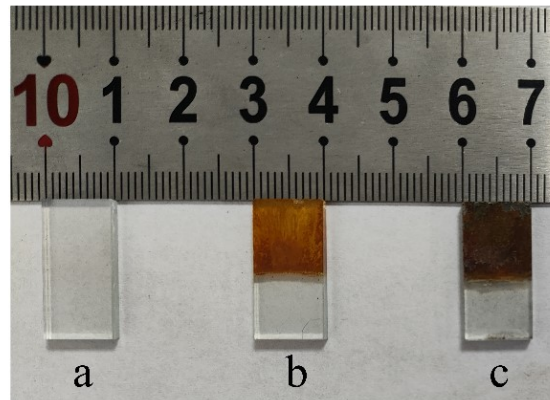


Fig. S6 The electrode pictures of (a) FTO, (b) NiFe(OH)_y/FTO, (c) NiS_x@NiFe(OH)_y/FTO.

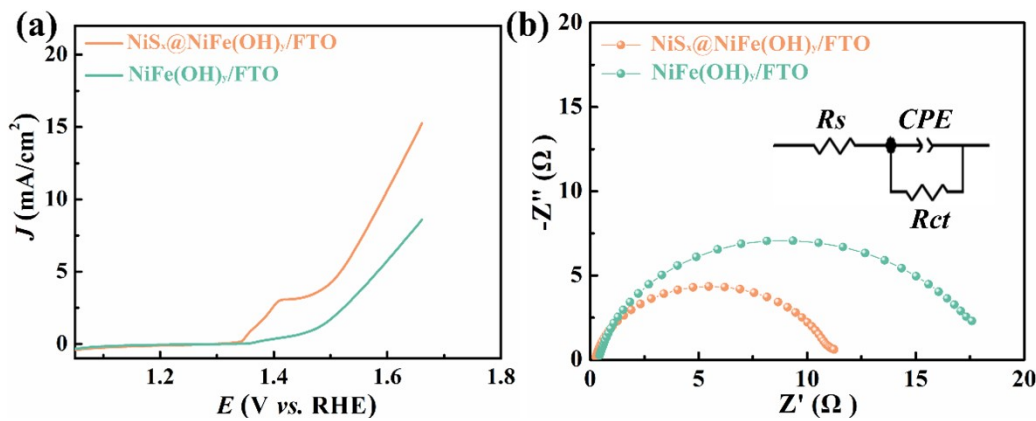


Fig. S7 OER performance of $\text{NiFe(OH)}_y/\text{FTO}$ and $\text{NiS}_x@\text{NiFe(OH)}_y/\text{FTO}$: (a) LSV curves, (b) EIS spectra.

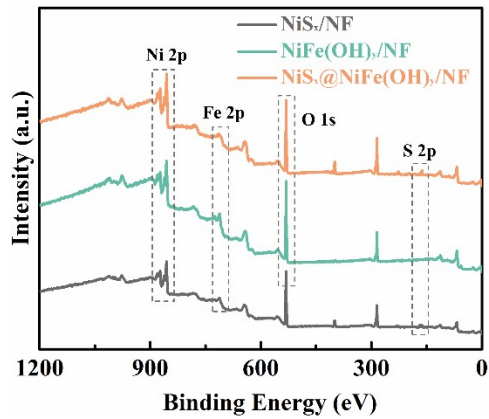


Fig. S8 survey XPS scan of NiS_x@NiFe(OH)_y/NF, NiFe(OH)_y/NF and NiS_x/NF.

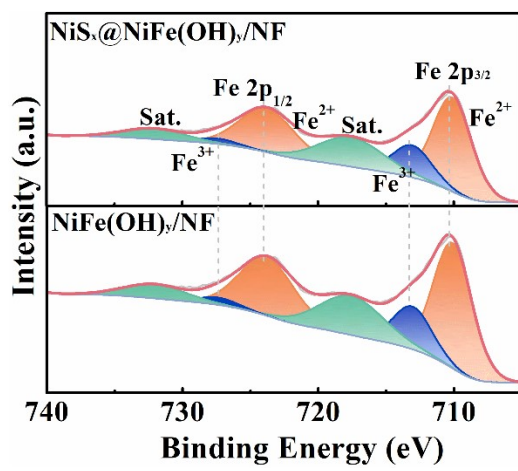


Fig. S9 High-resolution XPS comparison of Fe 2p for $\text{NiS}_x@\text{NiFe}(\text{OH})_y/\text{NF}$ and $\text{NiFe}(\text{OH})_y/\text{NF}$.

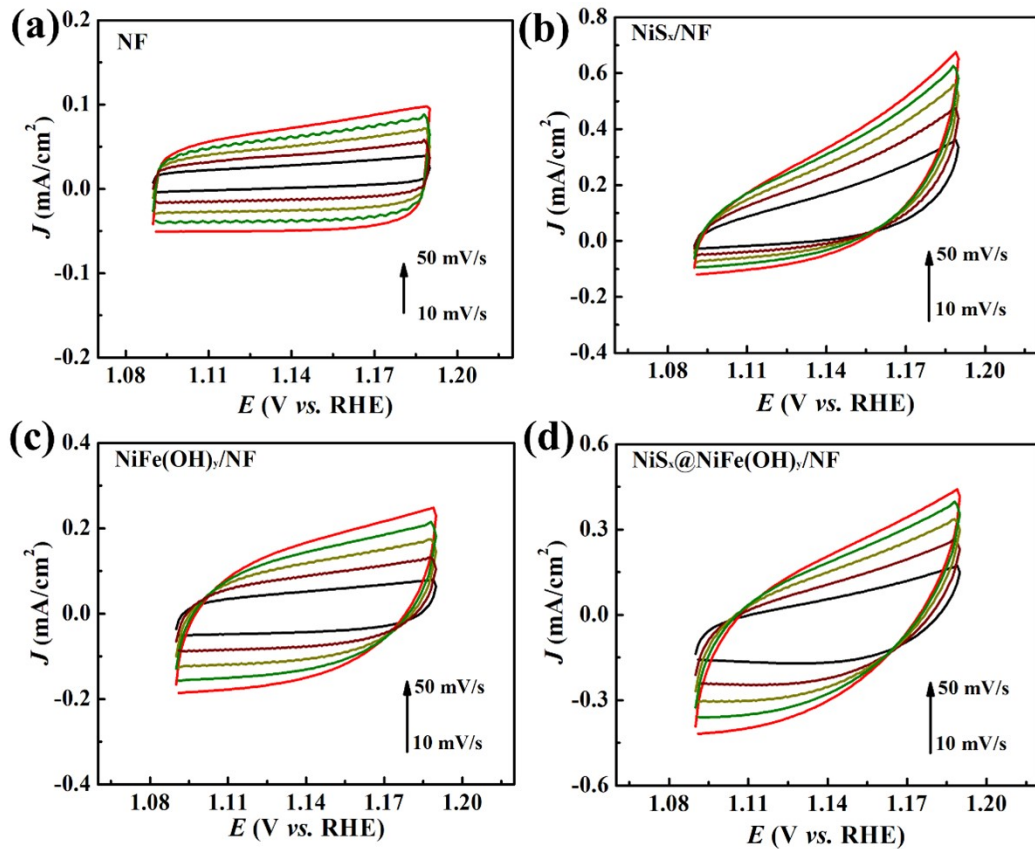


Fig. S10 CV curves of (a) NF, (b) NiS_x/NF , (c) $\text{NiFe(OH)}_y/\text{NF}$ and (d) $\text{NiS}_x@\text{NiFe(OH)}_y/\text{NF}$ at different scan rates (10, 20, 30, 40, and 50 mV/s).

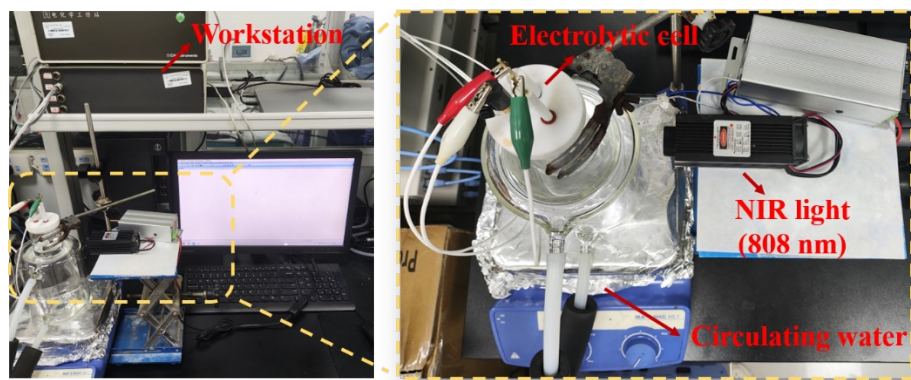


Fig. S11 The device picture of photothermal effect assist OER.

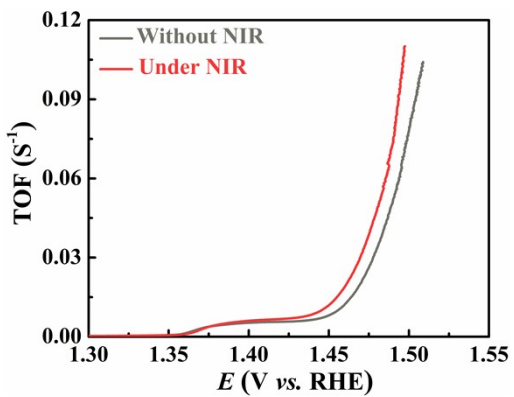


Fig. S12 TOF values of $\text{NiS}_x@\text{NiFe}(\text{OH})_y/\text{NF}$ under and without NIR light.

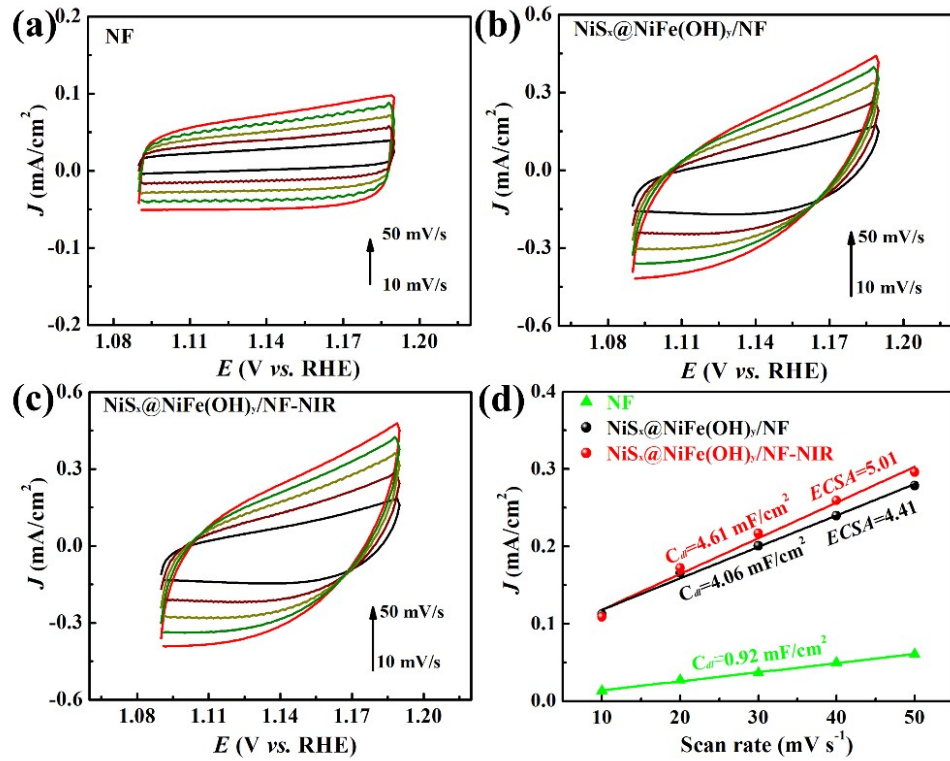


Fig. S13 CV curves of (a) NF, (b) NiS_x@NiFe(OH)_y/NF, (c) NiS_x@NiFe(OH)_y/NF-NIR at different scan rates (10, 20, 30, 40, and 50 mV/s). (d) ECSA data of NiS_x@NiFe(OH)_y/NF and NiS_x@NiFe(OH)_y/NF-NIR.

at different scan rates (10, 20, 30, 40, and 50 mV/s). (d) ECSA data of NiS_x@NiFe(OH)_y/NF and NiS_x@NiFe(OH)_y/NF-NIR.

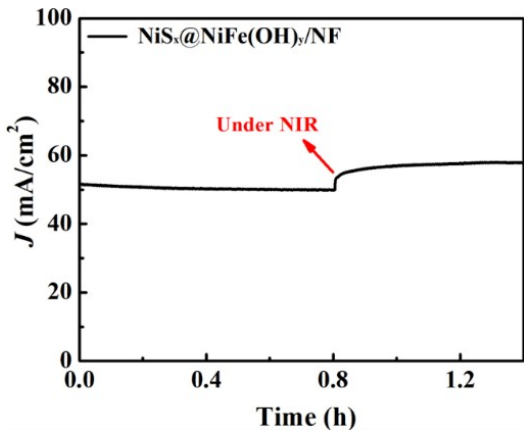


Fig. S14 J - T curves of $\text{NiS}_x@\text{NiFe}(\text{OH})_y/\text{NF}$ at 1.6 V vs. RHE under and without NIR light.

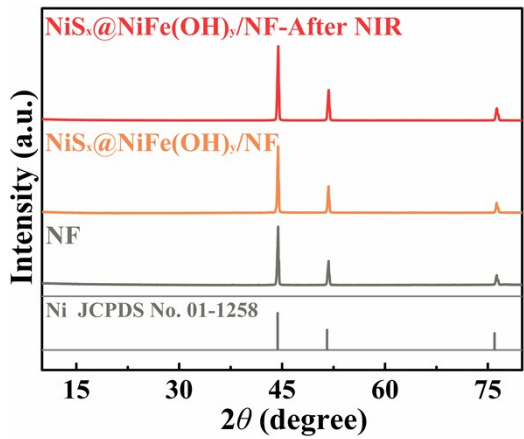


Fig. S15 XRD patterns of $\text{NiS}_x@\text{NiFe}(\text{OH})_y/\text{NF}$ after $J-T$ test under NIR light (NiS_x@NiFe(OH)_y/NF-After NIR), NiS_x@NiFe(OH)_y/NF and NF.

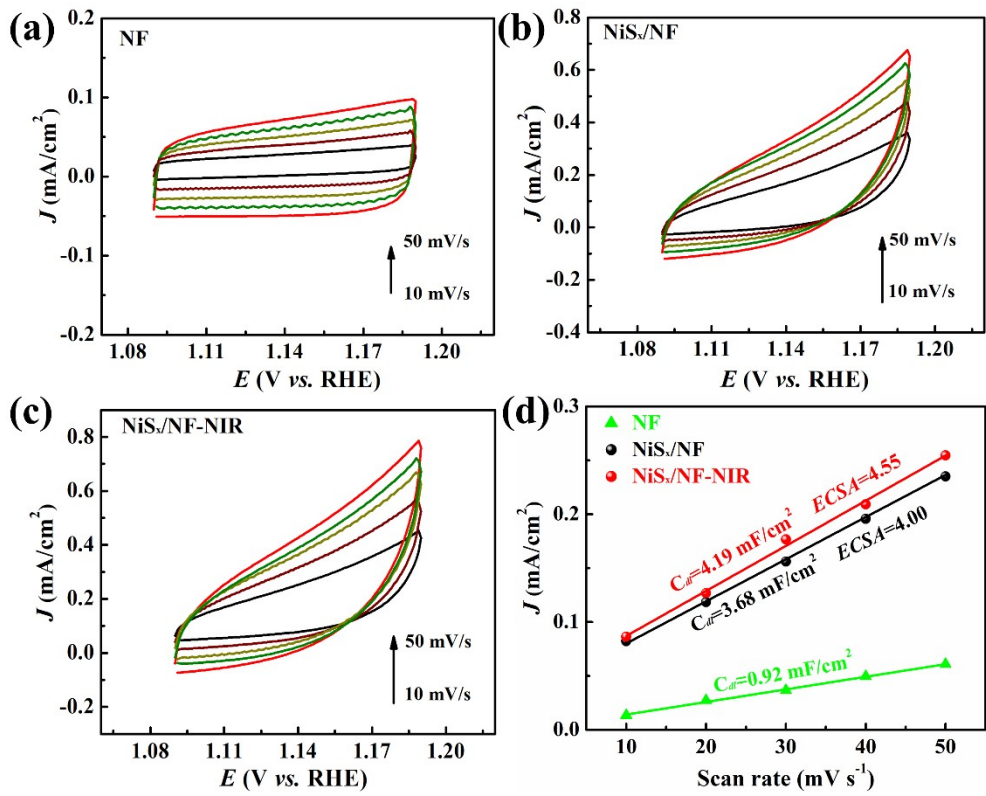


Fig. S16 CV curves of (a) NF, (b) NiS_x/NF, (c) NiS_x/NF-NIR at different scan rates (10, 20, 30, 40, and 50 mV/s). (d) ECSA data of NiS_x/NF and NiS_x/NF-NIR.

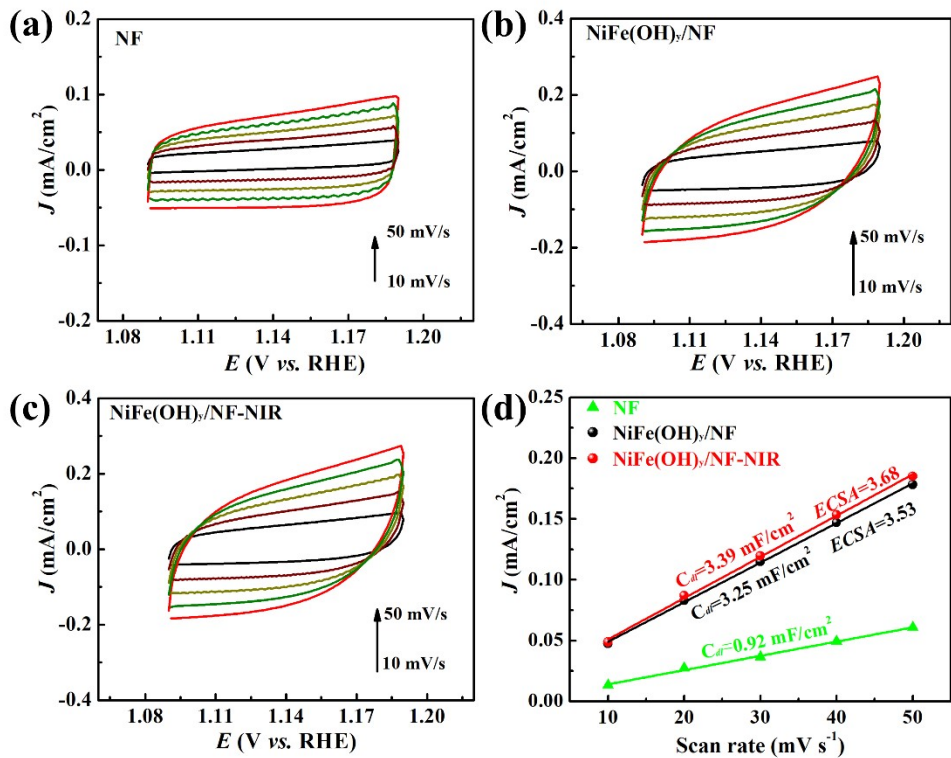


Fig. S17 CV curves of (a) NF, (b) NiFe(OH)_y/NF, (c) @NiFe(OH)_y/NF-NIR at different scan rates (10, 20, 30, 40, and 50 mV/s). (d) ECSA data of NiFe(OH)_y/NF and NiFe(OH)_y/NF-NIR.

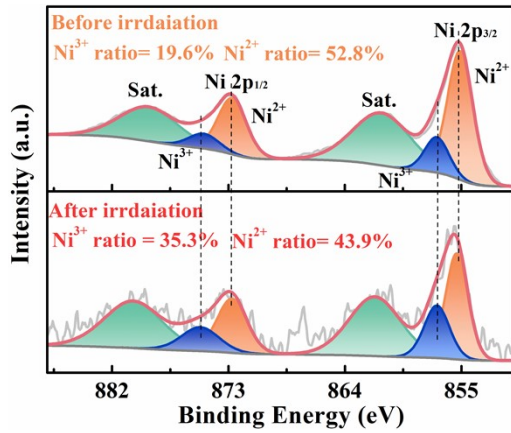


Fig. S18 High-resolution XPS comparison of Ni 2p in $\text{NiS}_x@\text{NiFe}(\text{OH})_y/\text{NF}$ before and after NIR light irradiation.

Table S1 Tafel slope comparison of $\text{NiS}_x@\text{NiFe(OH)}_y/\text{NF}$ to recently reported NiFe-based

Electrocatalysts for OER.

Electrocatalyst	Tafel slope (mV dec ⁻¹)	Testing condition	Reference
$\text{NiS}_x@\text{NiFe(OH)}_y/\text{NF}$	38.0	1.0 M KOH+NIR light	This work
$\text{NiS}_x@\text{NiFe(OH)}_y/\text{NF}$	45.1	1.0 M KOH	This work
$\text{Ni}_{0.3}\text{Fe}_{0.7}\text{-LDH}@\text{NF}$	56.68	1.0 M KOH	[1]
NiS/LDH/NF-5	61.2	1.0 M KOH	[2]
NiFeB	31.13	1.0 M KOH	[3]
NiFe/NiFeOOH	65.0	1.0 M KOH	[4]
A-NiFe NS/CuS	41	1.0 M KOH	[5]
$\text{Fe}_2\text{O}_3/\text{Fe}_{0.64}\text{Ni}_{0.36}@\text{C}-800$	82.98	1.0 M KOH	[6]
NiFe@C	87.6	1.0 M KOH	[7]
NiFe 2-1	58.6	1.0 M KOH	[8]
NiFe/NiFe:Pi	38	1.0 M KOH	[9]
fcc-Ni ₃ Fe/C	72	1.0 M KOH	[10]
$\text{Ni}_5\text{P}_4/\text{NiP}_2/\text{NiFe LDH}$	46.6	1.0 M KOH	[11]
$\text{NiFe(OH)}_x/\text{NiFe-MOF}$	52.05	1.0 M KOH	[12]
NiFe/NiFe-OH	41	1.0 M KOH	[13]
NiFe alloy	51.9	1.0 M KOH	[14]
$\text{FeOOH}@\text{Fe}_2\text{O}_3@\text{Ni(OH)}_2/\text{NF}$	60.15	1.0 M KOH	[15]
NiFe-HD/pre-NF	81	1.0 M KOH	[16]

Table S2. Fitted Values of the Equivalent Circuit Shown in **Fig. 2d** and **Fig. 4c**.

Electrode	R_s (Ω)	R_{ct} (Ω)	CPE
NF	2.52 (0.45)	3.17 (0.97)	0.02 (3.27)
NiS_x/NF	2.37 (0.41)	1.15 (2.06)	0.13 (4.51)
$\text{NiFe(OH)}_y/\text{NF}$	2.60 (0.49)	0.61 (3.38)	0.08 (8.41)
$\text{NiS}_x@\text{NiFe(OH)}_y/\text{NF}$	2.14 (0.43)	0.50 (4.39)	0.24 (8.91)
$\text{NiS}_x@\text{NiFe(OH)}_y/\text{NF-NIR}$	2.10 (0.34)	0.44 (3.63)	0.22 (8.02)

Table S3 The oxygen generation rate on $\text{NiS}_x@\text{NiFe(OH)}_y/\text{NF}$ in 1.0 M KOH at 1.6 V *vs.* RHE for 8 h in the presence and absence of NIR light irradiation (808 nm, 2 W cm⁻²).

Electrocatalyst	N_{O_2} (mmol h ⁻¹)
$\text{NiS}_x@\text{NiFe(OH)}_y/\text{NF}$	0.58
$\text{NiS}_x@\text{NiFe(OH)}_y/\text{NF-NIR}$	0.44

References

- (1) Y. Zhai, X. Ren, Y. Sun, D. Li, B. Wang and S. Liu, *Appl. Catal. B*, 2023, **323**, 122091.
- (2) Z. Wang, X. Mou, D. Li, C. Song and D. Wang, *Int. J. Hydrot. Energy*, 2022, **47**, 38124-38133.
- (3) H. Liao, G. Ni, P. Tan, Y. Liu, K. Chen, G. Wang, M. Liu and J. Pan, *Appl. Catal. B*, 2022, **317**, 121713.
- (4) D. Peng, C. Hu, X. Luo, J. Huang, Y. Ding, W. Zhou, H. Zhou, Y. Yang, T. Yu, W. Lei and C. Yuan, *Small*, 2022, **19**, 2205665.
- (5) H. Gao, W. Sun, X. Tian, J. Liao, C. Ma, Y. Hu, G. Du, J. Yang and C. Ge, *ACS Appl. Mater. Interfaces*, 2022, **14**, 15205-15213.
- (6) F. Zhou, M. Gan, D. Yan, X. Chen and X. Peng, *Small*, 2023, **19**, 2208276.
- (7) X. Wu, F. Yang and G. Shen, *Int. J. Hydrot. Energy*, 2022, **47**, 18955-18962.
- (8) X. An, Q. Hu, W. Zhu, L. Liu, Y. Zhang and J. Zhao, *Appl. Phys. A*, 2021, **127**: 865.
- (9) Y. Li and C. Zhao, *ACS Catal.*, 2017, **7**, 2535-2541.
- (10) G. Wei, Y. Shen, X. Zhao, Y. Wang, W. Zhang and C. An, *Adv. Funct. Mater.*, 2021, **32**, 2109709.
- (11) L. Yu, H. Zhou, J. Sun, I. K. Mishra, D. Luo, F. Yu, Y. Yu, S. Chen and Z. Ren, *J. Mater. Chem. A*, 2018, **6**, 13619-13623.
- (12) D. Liu, H. Xu, C. Wang, C. Ye, R. Yu and Y. Du, *J. Mater. Chem. A*, 2021, **9**, 24670-24676.
- (13) W. Zhu, W. Chen, H. Yu, Y. Zeng, F. Ming, H. Liang and Z. Wang, *Appl. Catal. B*, 2020, **278**, 119326.
- (14) D. Lim, E. Oh, C. Lim, S. E. Shim and S. H. Baeck, *Catal. Today*, 2020, **352**, 27-33.
- (15) M. Tang, X. Liu, A. Ali, Y. He, P. Shen and Y. Ouyang, *J. Colloid Interface Sci.*, 2023, **636**, 501-511.
- (16) B. Wu, Z. Yang, X. Dai, X. Yin, Y. Gan, F. Nie, Z. Ren, Y. Cao, Z. Li and X. Zhang, *Dalton Trans.*, 2021, **50**, 12547-12554.